Dynamics of Ionic Lipophilic Probes in Micelles: Picosecond Fluorescence Depolarization Measurements

ARTICLE *in* THE JOURNAL OF PHYSICAL CHEMISTRY · MAY 1993

Impact Factor: 2.78 · DOI: 10.1021/j100123a049

3 AUTHORS, INCLUDING:

E. L Quitevis
Texas Tech University
75 PUBLICATIONS **1,979** CITATIONS
SEE PROFILE

Andrew H Marcus
University of Oregon
81 PUBLICATIONS **1,377** CITATIONS
SEE PROFILE

Dynamics of Ionic Lipophilic Probes in Micelles: Picosecond Fluorescence Depolarization Measurements

Edward L. Quitevis,*,† Andrew H. Marcus,‡ and Michael D. Fayer*,‡

Department of Chemistry and Biochemistry, Texas Tech University, Lubbock, Texas 79409, and Department of Chemistry, Stanford University, Stanford, California 94305

Received: January 7, 1993; In Final Form: March 9, 1993

Time-resolved fluorescence anisotropies of two ionic lipophilic probes, merocyanine 540 and octadecylrhodamine B, in alcohol solvents and in sodium dodecyl sulfate, dodecyltrimethylammonium bromide, and Triton X-100 micelles were measured using time-correlated single-photon counting. In alcohols, the anisotropy decays were single exponentials. In micelles, the anisotropy decays were biexponential, corresponding to a short and a long rotational correlation time. The results are interpreted in terms of a two-step model consisting of fast restricted rotation of the probe and slow lateral diffusion of the probe in the micelle. The decrease in the residual anisotropy is caused mainly by lateral diffusion of the probe in the micelle. Information about the restricted rotation of the probe is obtained by using the parameters in the biexponential fit to calculate cone angles and wobbling diffusion constants for the wobbling-in-cone model. Lateral diffusion constants are also determined.

1. Introduction

A considerable amount of research has been directed toward understanding the structure and dynamics of micelles.[1,2] Because of the similarities between micelles and biological membranes, they have served as model systems. They act as unique media for chemical reactions and excitation energy transport studies. Aqueous micellar solutions have been successfully used as mobile phases in high-performance liquid chromatography, gel permeation chromatography, thin-layer chromatography, and electrokinetic chromatography.[3] In order to fully exploit micelles in these applications, the dynamics of molecules in micelles must be understood.

Fluorescence depolarization (FDP) is a technique that is widely used to study the dynamics in micelles and lipid bilayers.[4] It is a particularly useful technique, because of its sensitivity to membrane order and fluidity. In time-resolved FDP, one measures the fluorescence anisotropy $r(t)$, which is given by the time correlation function[5]

$$r(t) = (2/5)\langle P_2[\mu_e(t)\cdot\mu_a(0)]\rangle \qquad (1)$$

where μ_a and μ_e are the unit vectors corresponding to the transition dipoles for absorption of the excitation and emission of the fluorescence, $P_2(x)$ is the second Legendre polynomial, and the angle brackets represent an ensemble average. Information about the molecular dynamics of the probe in the membrane is contained in the time dependence of the correlation function.

The rotational diffusion of fluorescent probes attached to micelles has been previously studied.[6-16] These studies have primarily focused on probes that are either polycyclic aromatic hydrocarbons,[6-9,12,16b] xanthene dyes,[10,11,13] or oxazine dyes.[11,16a] Ionic lipophilic probes provide an opportunity to study the dynamics in a fairly well-defined region of the micelle. Ionic lipophilic molecules tend to be located near the surface of the micelle, with their polar ends positioned near the water–micelle interfacial region. The orientation of these probes in the micelle is well-defined. Because of hydrophobic interactions, the remaining portion of the molecule will point toward the hydrocarbon interior of the micelle and away from the water–micelle interface.

In this article, we describe a comparative time-resolved FDP study of two lipophilic fluorescent probes, merocyanine 540 (MC540) and octadecylrhodamine B (ODRB), in anionic sodium dodecyl sulfate (SDS) micelles, in cationic dodecyltrimethylammonium bromide (DTAB) micelles, and in nonionic Triton X-100 micelles. MC540 is an anionic lipophilic polymethine dye (Figure 1) which binds to biological and synthetic membranes.[17-22] The excited-state properties of MC540 are sensitive to electrical potential, and its fluorescence has been used to probe the transmembrane potential of many cell and organelle membranes.[23-26] The observation[27] that leukemia cells stained with MC540 are reduced by 5 orders of magnitude upon exposure to light has heightened interest in its photophysical and photochemical properties. The mechanism for the cytotoxic behavior of MC540, however, is controversial and remains an active area of research.[28-30] ODRB (Figure 1) is a cationic lipophilic fluorescent probe which has been used in studies of electronic excitation transport in micelles[31] and vesicles,[32] in distance determinations in biological complexes by resonance energy transfer,[33] and in the monitoring of cell fusion.[34]

MC540 is anchored to a micelle by the two tetramethylenic tails, with the benzoxazole end functionalized by the anionic sulfonate group situated at the surface of the micelle. For this orientation, MC540's transition moments are preferentially aligned along the normal to the surface of the micelle. Steady-state spectra confirm that the dye is localized near the micelle surface.[18,22b] Although negatively charged, MC540 binds readily to *anionic* SDS micelles.[22b] The driving force of the binding appears be the hydrophobic interactions of the two tetramethylenic tails which become embedded in the interior of the micelle. The dye should therefore bind to cationic and nonionic micelles with even greater efficacy. Similarly, ODRB is anchored to the interior of a micelle by the octadecyl chain, with the cationic xanthene moiety poised at the micelle surface.

The outline of this article is as follows. In section 2, we describe the preparation of the dye–micelle samples and the details of the FDP measurements. In section 3, we compare the observed anisotropy decays and show that the anisotropy decays are single exponentials in pure solvents but biexponentials in micelles. In section 4, the anisotropy decays for the micellar systems are described in terms of fast hindered rotational diffusion. Superimposed on this motion is the slow lateral diffusion of the probe

* Authors to whom correspondence should be addressed.
† Texas Tech University.
‡ Stanford University.

0022-3654/93/2097-5762$04.00/0

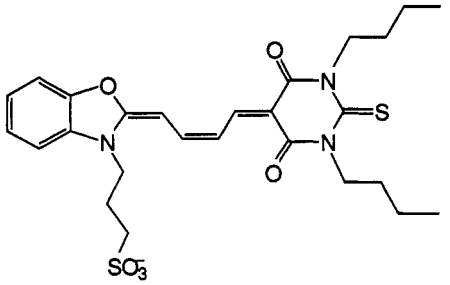

Merocyanine 540

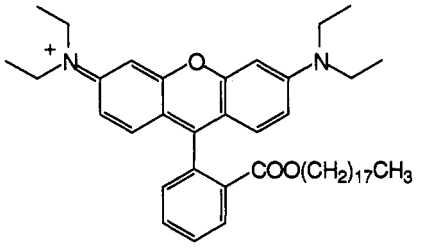

Octadecylrhodamine B

Figure 1. Structures of merocyanine 540 and octadecylrhodamine B. The counterions Na^+ and Cl^- are not shown.

in the micelle. Rotational diffusion of the micelles themselves is so slow that it makes a negligible contribution to the decays. This interpretation is based on a "two-step" model, which was previously developed to explain nuclear magnetic resonance (NMR) spin relaxation measurements of micelles. Lateral diffusion is the main cause of the anisotropy decay in these systems. The parameters in the two-step model are used to obtain cone angles and wobbling diffusion constants for the simple "wobbling-in-cone" model.

2. Experimental Details

MC540 (Sigma), ODRB (Molecular Probes), SDS (Sigma), DTAB (Sigma), and Triton X-100 (Sigma) were used without purification. Solvents of the highest commercial purity were used. MC540 was stored in the dark as a concentrated stock solution (1 mM) in a 1:1 volume mixture of ethanol and carbon tetrachloride. Samples were prepared by evaporating 100 μL of the stock solution and redissolving with 5 mL of solvent or an aqueous micellar solution. The final concentration was 20 μM.

The concentration of the micellar solutions was adjusted so that the dye-to-micelle ratio was ≤ 0.2. Under these conditions, the probability of having more than one dye molecule per micelle is low. This allowed us to neglect the effect of excitation energy transfer on the depolarization of the fluorescence. The micelle concentration [M] is given by

$$[M] = ([S] - \text{cmc})/N_{agg} \quad (2)$$

where [S] is the surfactant concentration, cmc is the critical micelle concentration, and N_{agg} is the mean aggregation number for the micelle. By substituting the values of cmc and N_{agg} listed in Table I into eq 2, we find that the desired micelle concentrations are obtained when [S] $\approx$ 20–30 mM. Also listed in Table I are the radii of the micelles.

The time-resolved FDP measurements were made by using time-correlated single-photon counting with excitation at 570 nm from a cavity-dumped and synchronously pumped rhodamine 6G dye laser. This wavelength corresponds to excitation at the red side of the absorption bands of these dyes. This avoids excitation of vibronic transitions, which can reduce the initial fluorescence anisotropy. The details of the apparatus[40] and the technique have been previously described.[41] Briefly, the laser pulse repetition rate was 823 kHz, and the laser pulse width was

TABLE I: Micelle Properties

micelle[a]	cmc,[b] mM	N_{agg}[b]	r_m, Å	τ_m,[f] ns
SDS	8.1	60	18[c]	5.9
DTAB	15.0	50	19[d]	6.9
Triton X-100	0.30	144	42[e]	74

[a] The micelle symbols are dodecyltrimethylammonium bromide (DTAB) and sodium dodecyl sulfate (SDS). [b] Values of the critical micelle concentration (cmc) and aggregation (N_{agg}) were obtained from refs 1, 3, and 35a. [c] Average of values given in refs 36 and 37. [d] Estimated by the method described in refs 38 and 39. [e] From ref 35. [f] The rotational correlation times of the micelles were calculated by using the Debye–Stokes–Einstein equation (eq 14) for a spherical micelle with radius r_m at 21 °C.

$\approx$10 ps. The fluorescence was collected from the front face of the sample and passed through a subtractive double monochromator set at 610 nm to a Hamamatsu microchannel plate detector. The instrument response function for this apparatus was $\approx$50-ps full width at half-maximum.

The detector polarizer was held fixed while the polarization of the excitation beam was rotated with a Pockel cell. The time-resolved fluorescence polarized parallel ($I_\parallel$) and perpendicular ($I_\perp$) to the polarization of the excitation beam was collected in an alternating manner under computer control for equal periods of time. This technique obviates the need to correct for the polarization bias of the detection system. The time-resolved fluorescence anisotropy $r(t)$ was calculated from these data by using the equation

$$r(t) = (I_\parallel - I_\perp)/(I_\parallel + 2I_\perp) \quad (3)$$

Data were collected until 10 000–20 000 counts were accumulated in the peak channel of the parallel fluorescence decay. The reproducibility was checked by comparing several data sets. To improve the signal-to-noise ratio, the data sets were averaged together.

The observed anisotropy decays were fit to the convolution of the instrument response with either a single-exponential or biexponential decay function using an iterative least-squares algorithm. The sum of the squared differences between the calculated $r(t)$ and the observed $r(t)$ was weighted by propagating the Poisson errors in the measured curves $I_\parallel$ and $I_\perp$. The quality of the fit was determined from the reduced χ^2 and by visual inspection of the fit and the data. All measurements were carried out at room temperature (21 $\pm$ 1 °C).

3. Results

Figures 2 and 3 show the fluorescence anisotropy decay of MC540 and ODRB in alcohol solvents. The anisotropy decay in these solvents provides a reference with which to compare the fluorescence anisotropy in micellar solutions. The anisotropy decay of these dyes in alcohols was fit by a single-exponential decay function

$$r(t) = r_0 \exp(-t/\tau_{rot}) \quad (4)$$

where r_0 is the anisotropy at zero time and τ_{rot} is the rotational correlation time for the probe in solution. The reduced χ^2 lies between 1.1 and 1.3 for these fits, indicating that a single exponential best describes the anisotropy decay for these dyes in solution. Table II lists the values of r_0 and τ_{rot}. τ_{rot} increased with solvent shear viscosity, with MC540 rotating slower than ODRB. Our value of τ_{rot} for MC540 in ethanol agrees with the previously reported value of 344 $\pm$ 30 ps.[42] Also listed in Table II are the values of the fluorescence lifetime τ_f, which were obtained from the slope of semilogarithmic plots of $I_\parallel + 2I_\perp$ vs time. The plots were linear over several orders of magnitude, indicating that the fluorescence decays of these dyes were single exponentials in alcohol solvents.

TABLE II: Fluorescence and Anisotropy Decay Parameters of Merocyanine 540 and Octadecylrhodamine B in Alcohols

solvent	η, cP	τ_f,[a] ps	r_0[b]	τ_{rot},[c] ps	χ^2/N[d]	τ_{rot}/η, ps cP^{-1}
			Merocyanine 540			
ethanol	1.14	456	0.342	326	1.2	286
1-butanol	2.60	712	0.350	750	1.18	288
1-heptanol	5.81	1000	0.315	1678	1.27	289
			Octadecylrhodamine B			
ethanol	1.14	2184	0.308	204	1.07	179
1-butanol	2.60	2568	0.338	489	1.27	188
1-heptanol	5.81	2774	0.335	1328	1.28	226

[a] Fluorescence lifetime obtained from the slope of semilogarithmic plot of $I_\parallel + 2I_\perp$ vs time. [b] Initial anisotropy. [c] Rotational correlation time. [d] Reduced χ^2 of fit to the anisotropy decay.

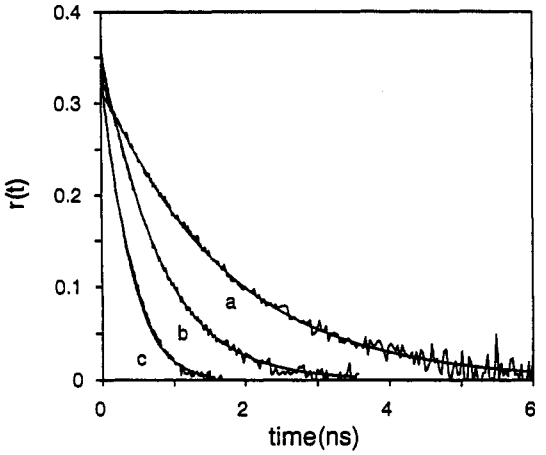

Figure 2. Fluorescence anisotropy decay of 20 μM merocyanine 540 in (a) 1-heptanol, (b) 1-butanol, and (c) ethanol. Solid lines are fits of data to a single exponential. Fit parameters listed in Table II.

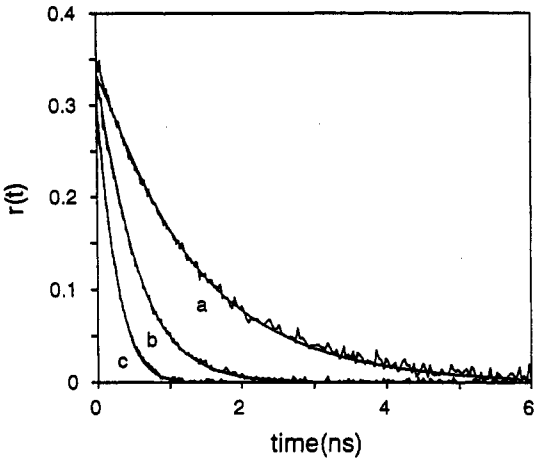

Figure 3. Fluorescence anisotropy decay of 20 μM octadecylrhodamine B in (a) 1-heptanol, (b) 1-butanol, and (c) ethanol. Solid lines are fits of data to a single exponential. Fit parameters listed in Table II.

The value of r_0 varied between 0.32 and 0.35 for MC540 and between 0.31 and 0.34 for ODRB. These values were less than the maximum possible value of 0.4, which would be observed if the absorption and emission moments were parallel. If the reduced value of r_0 is not caused by kinetics that are too rapid to resolve by single-photon counting, the initial anisotropy yields the angle ψ_{ae} between the emission and absorption dipoles through the equation

$$r_0 = 0.4P_2(\cos \psi_{ae}) \quad (5)$$

By using eq 5, we calculate that ψ_{ae} for both MC540 and ODRB is 19–20°.

Figures 4 and 5 illustrate the fluorescence anisotropy decays for MC540 and ODRB in micellar dispersions. In contrast to the anisotropy decay in alcohols, the anisotropy decay in micellar

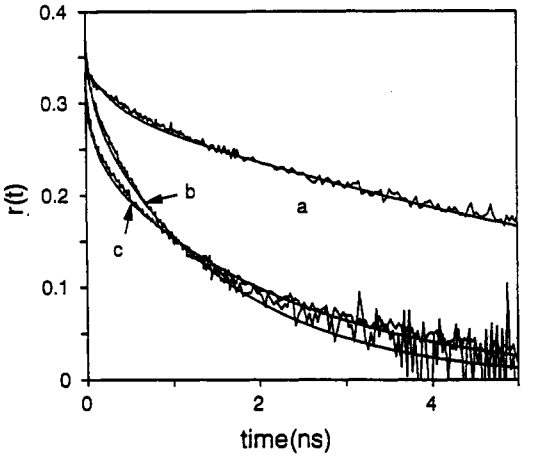

Figure 4. Fluorescence anisotropy decay of 20 μM merocyanine 540 in (a) 29 mM Triton X-100, (b) 20 mM SDS, and (c) 20 mM DTAB micellar solutions. Solid lines are fits of data to a biexponential decay function. Fit parameters listed in Table III.

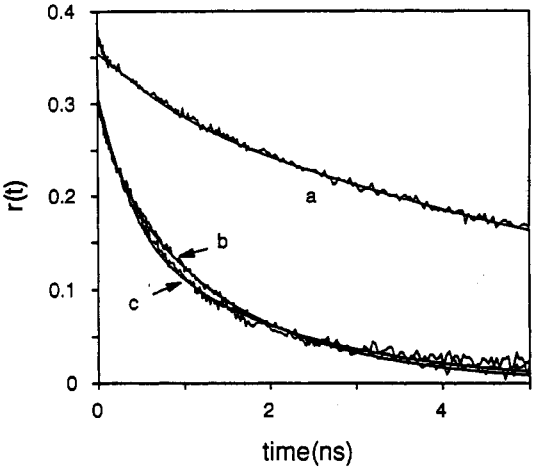

Figure 5. Fluorescence anisotropy decay of 20 μM octadecylrhodamine B in (a) 29 mM Triton X-100, (b) 20 mM DTAB, and (c) 20 mM SDS micellar solutions. Solid lines are fits of data to a biexponential decay function. Fit parameters listed in Table III.

dispersions was nonexponential. The anisotropy decays were fit by a biexponential function

$$r(t) = r_0[\alpha_1 \exp(-t/\tau_1) + \alpha_2 \exp(-t/\tau_2)] \quad (6)$$

Based on the value of the reduced χ^2 which ranged between 1.1 and 1.5 for these fits, we conclude that a biexponential adequately describes the time dependence of the measured $r(t)$. Table III lists the biexponential parameters corresponding to the fits. In micelles, the value of r_0 varied between 0.31 and 0.36 for MC540 and between 0.30 and 0.36 for ODRB. These values were within experimental error, the same as found in pure solvent. In all cases, the anisotropy decay was characterized by a fast component τ_1 and a slow component τ_2, with the long component dominating

TABLE III: Fluorescence and Anisotropy Decay Parameters of Merocyanine 540 and Octadecylrhodamine in Micelles

micelle	τ_f,[a] ps	r_0[b]	τ_1,[c] ps	τ_2,[c] ps	α_1[c]	α_2[c]	$\langle\tau_{corr}\rangle$,[d] ps	χ^2/N[e]
				Merocyanine 540				
SDS	560	0.355	91	1610	0.214	0.786	1285	1.46
DTAB	1224	0.310	102	2267	0.223	0.777	1784	1.20
Triton X-100	1760	0.340	246	8550	0.129	0.871	7479	1.16
				Octadecylrhodamine B				
SDS	2240	0.315	275	1902	0.451	0.549	1168	1.53
DTAB	1760	0.300	195	1527	0.242	0.758	1205	1.09
Triton X-100	2800	0.355	727	7753	0.311	0.689	5568	1.12

[a] Fluorescence lifetime obtained from the average slope of semilogarithmic plot of $I_\parallel + 2I_\perp$ vs time. [b] Initial anisotropy. [c] Biexponential parameters for fit of anisotropy (eq 6). [d] Average rotational correlation time (eq 7b). [e] Reduced χ^2 of fit to anisotropy decays.

the decay, i.e., $\alpha_2 > \alpha_1$. For MC540, the ratio of the slow and the fast components, τ_2/τ_1, was ≈18–20 in SDS and DTAB micelles and ≈35 in Triton X-100 micelles. In contrast, the ratio was smaller for ODRB: $\tau_2/\tau_1 \approx 7$–8 in SDS and DTAB micelles and ≈11 in Triton X-100. The average correlation time $\langle\tau_{corr}\rangle$ can be roughly used to compare the anisotropy decays, because it is model independent. The average correlation time is defined as

$$\langle\tau_{corr}\rangle = \frac{1}{r_0}\int_0^\infty r(t)\,dt \tag{7a}$$

Therefore, for a biexponential anisotropy decay, the average is simply given by

$$\langle\tau_{corr}\rangle = \alpha_1\tau_1 + \alpha_2\tau_2 \tag{7b}$$

The values of $\langle\tau_{corr}\rangle$ listed in Table III show that the anisotropy decay in micellar solution was slower for MC540 than for ODRB. For both MC540 and ODRB, reorientation occurred on similar time scales in DTAB and SDS micellar solutions and was roughly 5 times slower in Triton X-100 micellar solution. These trends are evident from the curves illustrated in Figures 4 and 5. A biexponential anisotropy decay was previously observed for ODRB in Triton X-100 micelles by Visser et al.[15] Although our value of τ_2 agrees with their value of 8.8 ± 0.2 ns, our value of τ_1 is considerably less than their value of 2.0 ± 0.2 ns. Their longer value of τ_1 could be the result of using a reference method and global analysis of $I_\parallel$ and $I_\perp$, with the reference being rose bengal in water, to obtain the anisotropy parameters. Also listed in Table III are the fluorescence lifetimes, which were obtained from semilogarithmic plots of $I_\parallel + 2I_\perp$ vs time. The plots showed slight deviations from linearity. The lifetimes listed in Table III were therefore calculated from the average slope of these plots.

4. Discussion

A. Rotational Diffusion in Alcohols. In principle, the anisotropy decay is given by the sum of five exponentials.[43,44] The fact that the anisotropies were well fitted by single exponential decay functions suggests that these dyes can be modeled by ellipsoids or spheres for the purposes of determining their reorientational dynamics. For MC540, a prolate ellipsoid has been found to best describe its shape from the point of view of its reorientational dynamics in solution.[42,45] The values of τ_{rot}/η listed in Table II were the same for all the alcohols. Based on the Debye–Stokes–Einstein (DSE) equation,[46] this ratio is equal to the effective hydrodynamic volume divided by k_BT, where k_B is Boltzmann's constant and T is the absolute temperature. The lack of variation of τ_{rot}/η with solvent is consistent with picosecond pump–probe measurements of the ground-state rotational diffusion of MC540 in polar solvents[45] and confirms that the reorientational dynamics of the dye are well described by the DSE equation.

Despite ODRB's wide usage in membrane and energy-transfer studies, its reorientational dynamics in solution has not been well studied. The fact that the fluorescence anisotropy decay was a single exponential suggests that ODRB can be described by a simple rotor from the point of view of rotational diffusion in solution. If the octadecyl group is fully extended, the shape of the molecule can be approximated by a prolate ellipsoid. However, if the octadecyl group is coiled, the shape of the molecule can be approximated by a sphere. Either type of rotor would give rise to a single-exponential anisotropy decay. Although the values of τ_{rot}/η are similar (Table II), the variation in τ_{rot}/η with solvent indicates that its rotational diffusion cannot be completely explained by the DSE equation. The ratio increases with the length of the hydrocarbon portion of the alcohol solvent. It is possible that the average conformation of the ODRB octadecyl alkyl chain changes with solvent. Other possibilities are that the variations are caused by a difference in the dielectric friction[47–49] or changes in the boundary conditions[50] with solvent.

B. Rotational Diffusion in Micelles. In micellar systems, the observation of two distinctly different correlation times in the anisotropy decay implies the existence of two dynamical processes that occur on different time scales. One obvious possibility is that the short and long components in the anisotropy decay arise, respectively, from the rotational diffusion of free dye in solution and micelle-bound dye. This explanation was used previously to rationalize the rotational diffusion of xanthene and oxazine dyes in micelles.[11] If the partitioning between water and micelle were correct, the ratio α_1/α_2 would then give the ratio of free dye to micelle-bound dye. This can be separately checked by estimating the ratio of the equilibrium concentrations. The addition of MC540 to micelles can be considered to arise from the binding to a set of identical and independent sites with an intrinsic equilibrium constant K_a given by

$$K_a = [M][D]/[C] \tag{8}$$

where [M], as discussed above, is the concentration of micelles, [D] is the concentration of free dye, and [C] is the concentration of dye–micelle complexes. The value of K_a in recent binding studies of MC540 to SDS micelles was found to be equal to 7 ± 1 μM.[22a] Using this value of K_a, we estimate that the ratio of free MC540 to micelle-bound MC540 at a total dye concentration of 20 μM is 0.035. This ratio is roughly 10 times smaller than the ratio of 0.272 calculated from the values of α_1 and α_2 listed in Table II. Given that SDS micelles are negatively charged, the ratio of free dye to micelle-bound dye should even be smaller for MC540 bound to positively charged DTAB micelles and to nonionic Triton X-100 micelles. The value of the ratio α_1/α_2 is 0.287 for MC540 in DTAB micelles and 0.148 for MC540 in Triton X-100 micelles. These large values of α_1/α_2 are inconsistent with the concentration ratio estimated from K_a. In addition, the fluorescence decay time at short times did not differ from the decay time at longer times. The observed anisotropy decays for MC540 must therefore be largely attributed to dye bound to micelles. Although equilibrium binding studies have not been performed for ODRB in micelles, the similarity of the values of α_1/α_2 for ODRB and MC540 suggests that the anisotropy decay of ODRB in micelles is also due to the dynamics of the dye bound to micelles. Ediger et al.[31a] studied rhodamine B (RB) and ODRB

in Triton X-100 and found that for RB, 50% of the fast component was due to rotation in water. In contrast, ODRB did not show this, indicating that none of the ODRB was in water. Furthermore, although the fluorescence decays deviated slightly from monoexponential behavior, they were clearly not biexponential.

Another possible explanation is that the anisotropy decay is caused by the rotational diffusion of the dye bound to two different sites within the micelle. These two solubilization sites correspond to "the hydrophobic dissolved state" (i.e., the core) and the more polar "adsorbed state" near the micelle surface.[51,52] This two-site model would imply that the correlation times τ_1 and τ_2 measure the rigidity or the microviscosity of these two sites and that the coefficients α_1 and α_2 correspond to the relative probabilities of finding the dye in these two sites. To see what picture would be implied by this two-site model, we will consider MC540 in DTAB micelles. Based on the values of τ_1 and τ_2 listed in Table II, the microviscosity in one site is $\approx$22 times higher than in the other site. Furthermore, based on the values of α_1 and α_2 listed in Table II, the probability of finding the dye in this more viscous site is 3.7 time greater. In micelles, the region of high microviscosity is found in the interior of the micelle.[6] Therefore, we would conclude that the probability of finding the probe molecules is highest in the interior of the micelle. This is not physically reasonably because the dye is charged and should be at the surface of the micelle. Similar arguments can be made for ODRB. In addition, very detailed studies of electronic excitation transport among ODRB molecules in Triton X-100 micelles show that the ODRB molecules are at the surface.[31]

The biexponential anisotropy decay is therefore not the result of a distribution of probe sites but instead is a manifestation of the motion of the probe species in the micelle. Within the anisotropic rotational diffusion model, anisotropy decays that are biexponential can be obtained in the case of symmetric rotors.[43,44] For example, the biexponential anisotropy decay for perylene in solution can be explained by this model.[53] However, the observation of single-exponential decays for both probe molecules in the three alcohol solvents is antithetical to this explanation. It is extremely unlikely that the molecular structures of MC540 and ODRB will change to such a great extent upon entering the micelles that the new structures give rise to the biexponential decays.

C. Two-Step Model. Probes bound to lipid bilayer membranes exhibit a partial orientational relaxation. In these systems, the fluorescence anisotropy of the probe is a maximum at the moment of excitation and decays to a constant value after a period of time. This behavior is a signature of hindered or restricted rotational diffusion.[54-58] If the probe is bound to the micelle in the same way that probes are bound to lipid bilayer membranes, the motion of the probes in micelles should undergo similar motions. However, the anisotropy in micellar systems decays to zero at long times. There must hence be superimposed additional dynamics that reduce the residual anisotropy to zero.

The two-step model was first introduced to explain the results from nuclear magnetic resonance measurements of micelles.[59,60] ^{13}C T_1 relaxation and the nuclear Overhauser enhancement (NOE) have been extensively used to probe the dynamics of micelles.[61] In ^{13}C NMR, the relaxation of a protonated ^{13}C is determined by the dipolar interaction between the carbon nuclei with hydrogen nuclei, which fluctuate because of spatial motion. The relaxation time is determined by the reorientation of the ^{13}C–H vectors with respect to the magnetic field. The dipolar spin relaxation rate ($1/T_1$) and the NOE are given by expressions involving spectral densities, which are the Fourier transforms of time correlation functions describing the motional fluctuations that cause spin relaxation. In general, ^{13}C T_1 values in micellar systems are significantly shorter than those of a surfactant molecule in solution.[59,60] Furthermore, ^{13}C T_1 values in micellar systems vary with the strength of the magnetic field. This behavior is interpreted in terms of the two-step model. This model emphasizes the separation of fast internal motions within the micelle and slow motions on a time scale characteristic of the micelle dimension.

In the two-step model, the fast and slow motions are assumed to be separable. If the two motions are independent, the total correlation function will be rigorously given by the product of two correlation functions corresponding to the fast motion within the micelle and to the slow motion of the micelle:[55a,c]

$$C_T(t) = C_{fast}(t)C_{slow}(t) \tag{9}$$

If the slow motion is isotropic, the corresponding correlation function will decay as a single exponential

$$C_{slow}(t) = \exp(-t/\tau_{slow}) \tag{10}$$

where τ_{slow} is the rotational correlation time corresponding to the slow motion. Spin relaxation studies have shown that τ_{slow} contains contributions from both the rotational motion of the micelle and the lateral diffusion of the monomers over the curved surface of the micelle.[59,60] The rotational correlational time is then given by

$$\frac{1}{\tau_{slow}} = \frac{1}{\tau_m} + \frac{1}{\tau_D} \tag{11}$$

where τ_m is the correlation time corresponding to the rotation of the whole micelle and τ_D is the correlation time corresponding to the lateral diffusion of the monomers in the micelle.

The fast motion is modeled as restricted rotational diffusion. In general, the correlation function for restricted rotational diffusion can be written as

$$C_{fast}(t) = (1 - S^2)\exp(-t/\tau_e) + S^2 \tag{12}$$

where S is a generalized order parameter and τ_e is an effective correlation time. The rationale for this correlation function is the following. Because the surfactant molecules are anchored at the micelle–water interface, the motion of a segment of an alkyl chain is not isotropic. Hence, the ^{13}C–H vector does not sample all directions with respect to the magnetic field.

Combining eqs 11 and 12 gives the total correlation function as

$$C_T(t) = (1 - S^2)\exp(-t/\tau_{fast}) + S^2\exp(-t/\tau_{slow}) \tag{13a}$$

with

$$\frac{1}{\tau_{fast}} = \frac{1}{\tau_e} + \frac{1}{\tau_{slow}} \tag{13b}$$

Lipari and Szabo[55] have shown that the numerical value of S^2, which is a measure of the spatial restriction of the motion, and τ_e, which is a measure of the rate (time scale) for the motion, can be defined in a model-independent way. The order parameter S satisfies the inequalities $0 \le S^2 \le 1$. If the fast motion is isotropic, $S = 0$, and if it is completely restricted, $|S| = 1$.

D. Two-Step Model and Fluorescence Anisotropy. The two-step model for dipole-spin relaxation can be readily adapted to describe the anisotropy decay in micelles. Dipolar relaxation and FDP are analogous in that the ^{13}C–H vectors play the same role as the absorption and emission dipoles.[55a] Indeed, eq 13a reproduces the observed time dependence of the fluorescence anisotropy decay in our systems, with the first and second terms of eq 13a corresponding, respectively, to the fast and slow components of the biexponential fits to the data.

Based on the two-step model, τ_2 contains contributions from the rotational motion of the micelle, τ_m, and the lateral diffusion of the probe in the micelle, τ_D. The value of τ_m can be calculated from the DSE equation[46] by assuming a spherical micelle rotating

TABLE IV: Two-Step Model and Wobbling-in-Cone Model Parameters

micelle	τ_e,[a] ps	$\|S\|$[b]	τ_D,[c] ns	D_L,[d] 10^{-6} cm^2 s^{-1}	θ_0[e]	D_w,[f] 10^8 s^{-1}
			Merocyanine 540			
SDS	96	0.887	2.2	3.8	22.7°	4.8
DTAB	107	0.881	3.4	2.7	23.3°	4.5
Triton X-100	253	0.933	9.7	4.5	17.3°	1.1
			Octadecylrhodamine B			
SDS	321	0.741	2.8	2.8	35.3°	3.4
DTAB	223	0.871	2.0	4.5	24.3°	2.4
Triton X-100	802	0.830	8.7	5.1	28.1°	0.87

[a] Effective correlation time for restricted rotational diffusion (eq 12). [b] Generalized order parameter (eq 12). [c] Lateral diffusion time (eq 15). [d] Lateral diffusion constant (eq 16). [e] Cone angle from wobbling-in-cone model (eq 18). [f] Wobbling diffusion constant (eq 21).

in water with sticking boundary conditions:

$$\tau_m = \frac{4\pi r_m^3 \eta}{3k_B T} \tag{14}$$

where r_m is the radius of the micelle and η is the solvent shear viscosity of water, not the solution. Using the radii of the micelles listed in Table I and a viscosity of 0.98 cP for water at 21 °C, we calculate that the values of τ_m are 5.9, 6.9, and 74 ns for SDS, DTAB, and Triton X-100, respectively. Note that in all cases, these times are considerably longer then τ_2 (Table III). Therefore, τ_2 is dominated by lateral diffusion.

If this difference between τ_2 and τ_m is attributed to the lateral diffusion of the probe within the micelle, the correlation time for lateral diffusion can be obtained from τ_2 and τ_m by using the equation

$$\tau_D = \tau_2\tau_m/(\tau_m - \tau_2) \tag{15}$$

A comparison of the correlation times for lateral diffusion (Table IV) and the values of τ_2 shows that the main motion that causes the anisotropy to decay to zero in these micelles is lateral diffusion. The correlation time is related to the lateral diffusion constant by the equation

$$\tau_D = \frac{r_m^2}{4D_L} \tag{16}$$

The assumption behind eq 16 is that the chromophoric part of the probe is primarily localized at the surface of the micelle and the micelle is essentially spherical. Thus, one can view lateral diffusion of the chromophore in a micelle as the diffusion of a particle on the surface of a sphere of radius r_m.[62] This results in two-dimensional diffusion, giving rise to the factor of 4 in eq 16. The diffusional equation for lateral diffusion on a sphere reduces to an orientational diffusional equation, which is governed by a diffusion constant Θ, with $\Theta = D_L/r_m^2$. Equation 16 follows for isotropic orientational diffusion with the correlation time given by $\tau_D = (4\Theta)^{-1}$, in analogy to three-dimensional diffusion.[5] Visser et al.[15] rationalized the biexponential anisotropy decay for ODRB in Triton X-100 micelles and reversed AOT micelles in terms of an equation identical to eq 13a. However, they did not consider lateral diffusion and attributed the slow correlation time to only micellar rotation.

Interestingly, although the values of τ_D differ greatly between the micelles, the values of D_L (Table IV) calculated by using eq 16 do not. The lateral diffusion constants vary from 3×10^{-6} to 5×10^{-6} cm^2 s^{-1}. The variation in the values of τ_D occurs because τ_D scales with the square of the radius of the micelle. Although the lateral diffusion coefficients are known for the lateral diffusion of surfactant molecules in micelles, they are not known for these fluorescent probes. Based on NMR relaxation data,[60] lateral diffusion constants of surfactant molecules in micelles are in the range of $(0.2–1.5) \times 10^{-6}$ cm^2 s^{-1}. The lateral diffusion of these dyes is slightly faster than that of the surfactant molecules in these micelles. The rate of lateral diffusion in micelles is 100 times faster than in lipid bilayer membranes.[63] This can be attributed to a difference between the packing density of micelles and bilayer membranes. Because micelles are curved, the packing is less tight than in lipid bilayer layers. In models for lateral diffusion, molecules move by exchanging positions or by migrating through small gaps or interstitial sites in the membrane.[63,64] Consequently, in the context of these jump models, one expects the rate of lateral diffusion to be faster when the packing is less tight.

E. Wobbling-in-Cone Model. The order parameter gives information about the packing in the vicinity of the probe molecule. NMR relaxation data indicate a higher degree of order near the surface than in the interior of the micelle.[60] The high values of $|S|$ (>0.8 for MC540 and >0.7 for ODRB) are consistent with the assumption that the probe molecules are located at the micelle–water interface. For a given micelle, the value of $|S|$ is slightly higher for MC540 than for ODRB. On the basis of thermodynamic arguments, it was originally concluded that the interior of the micelle resembles a liquid hydrocarbon.[65,66] This conclusion is supported by spectroscopic observations[6,67,68] that show apolar probes, which favor the interior of the micelle, move in a liquidlike environment. Therefore, the rotational diffusion of MC540 or ODRB would be more isotropic (i.e., a low value of $|S|$) if these probes were buried in the interior of the micelle.

The order parameter is a measure of the average micelle structure near the probe. It contains no information about the dynamical properties. The dynamics are instead reflected in the relative values of τ_e. A comparison of the values of τ_e listed in Table IV reveals that the time scales for the fast internal motion of MC540 in SDS micelles and in DTAB micelles are similar. The values of τ_e were calculated from eq 13 by setting τ_1 and τ_2 equal to τ_{fast} and τ_{slow}, respectively. We can consider the effective correlation time to be a measure of the relaxation of the local structure. Because of intermolecular interactions between the probe and its local environment, τ_e really refers to the relaxation of a probe-perturbed local micelle structure. For MC540 and ODRB, the anisotropy probes interactions at the micelle–water interface. Since the alkyl chains are identical for DTAB and SDS, one would expect that electrostatic interactions should dominate the relaxation of local structure at the surface of the micelle. In other words, ODRB, being positively charged, should undergo a different motion in anionic SDS micelles than in cationic DTAB micelles. Indeed, there is a pronounced difference in τ_e for ODRB in SDS and in DTAB micelles. The relaxation time for ODRB is ≈44% longer in SDS micelles then in DTAB micelles. A rather simple explanation for this is that electrostatic attraction between the negatively charged head groups and the positively charged xanthene moiety causes the probe motions to be more strongly coupled to dynamics of the micelle, whereas in DTAB micelles, the electrostatic repulsion between the positively charged heads groups and the xanthene moiety reduces the coupling of the probe motions to the dynamics of the micelle. The value of τ_e is considerably larger in uncharged Triton X-100 micelles than in charged micelles. This implies that the local structure takes 3–4 times longer to relax in Triton X-100 micelles than in the charged SDS or DTAB micelles. In the case of MC540, τ_e is

essentially the same for MC540 in SDS and DTAB micelles. This suggests that MC540 protrudes out of the micelle and into the water region of the interface, thereby reducing its interactions with the head groups and allowing it to be less motionally restricted.

The usual approach to understanding the relationship between the anisotropy decay and the structure and dynamics of a membrane is to interpret τ_e and S in terms of specific models for restricted rotational diffusion.[54] The simplest models treat the probe as a symmetrical ellipsoid whose transition moment is aligned parallel to a symmetry axis. The probe is assumed to freely diffuse, with a wobbling constant D_w in a cone of semiangle θ_0. The correlation function for this motion is given exactly by an infinite series of exponentials.[54] This infinite series is well approximated by a single-exponential expression of the form of eq 12.

The difficulty in using the simple models is that the molecules must be rodlike with the transition moment either parallel or perpendicular to the long axis. As discussed previously, the reorientational dynamics of MC540 in polar solvents can be consistently described in terms of a prolate ellipsoid, with the long axis parallel to the trienyl backbone and the transition moment lying primarily along the backbone. Therefore, in the context of these models, MC540 can be approximated by a rodlike molecule with its transition moment parallel to the long axis.

For this type of rotor, the restricted motion can be described by the wobbling-in-cone model.[54] In this model, S^2 is given by

$$S^2 = \left[\tfrac{1}{2}(\cos\theta_0)(1+\cos\theta_0)\right]^2 \qquad (17)$$

where θ_0 is the cone angle measured from the normal to the micelle surface. θ_0 can be calculated from the values of $|S|$ by using eq 17. Specifically

$$\theta_0 = \cos^{-1}\{(1/2)[(1+8|S|)^{1/2}-1]\} \qquad (18)$$

if one assumes $0 \le \theta_0 \le 90°$. Table IV lists these angles for MC540 and ODRB. The semiangle for MC540 in SDS micelles is approximately the same as in DTAB micelles and is equal to $\approx 23°$. In contrast, a narrower cone is observed in Triton X-100 micelles: the semiangle is $\approx 17°$.

It is not clear, in the case of ODRB, whether the emission dipole moment is perpendicular or parallel to the surface normal. Johansson and Niemi[32] found in their excitation energy transport studies of ODRB in vesicles that the xanthene moiety is aligned in such a way that the emission moment is perpendicular to the surface normal. If this orientation is chosen for ODRB in micelles, the motion of the molecule is roughly represented by the motion of a rod-shaped molecule with its emission moment perpendicular to the long axis. For this orientation, the emission moment diffuses around the long axis of the molecule, as the long axis wobbles. This motion is described by the simple "spinning-in-equatorial-band" model. For this model, the motion is uniform over the equatorial band $\theta_0 \le \theta \le \pi - \theta_0$ and

$$S^2 = \left[\tfrac{1}{2}(1-\cos^2\theta_0)\right]^2 \qquad (19)$$

where $|S|$ cannot exceed 0.5. Given that the values of $|S|$ listed in Table IV are greater than 0.75, the spinning-in-equatorial-band model cannot be correct for ODRB. In contrast, in the wobbling-in-cone model, $|S|$ can have any value between 0 and 1. Since the values of $|S|$ for ODRB are greater than 0.5, ODRB behaves as if it were a rodlike molecule, with its transition dipole parallel to the long axis. In these micelles, the transition moment of ODRB is essentially aligned parallel to the long axis of the molecule. Such a conformation is possible because of the flexibility of the alkyl chain. The xanthene moiety can be oriented in such a way that the transition moment is aligned so that it is roughly parallel to the octadecyl chain. In many respects, this alignment is preferable because it allows a greater portion of hydrophobic regions of the xanthene ring to be embedded in the interior of the micelle. Using eq 18, we calculate that the cone angle for ODRB is larger than for MC540 and ranges from 24 to 35° (Table IV).

Lipari and Szabo[55] have shown that D_w, S^2, τ_e, and the cone angle are related to each other by the equation

$$D_w\tau_e(1-S^2) = -x_0^2(1+x_0)^2\{\ln[(1+x_0)/2] + (1-x_0)/2\}/[2(1-x_0)] + (1-x_0)(6+8x_0-x_0^2-12x_0^3-7x_0^4)/24 \qquad (20)$$

where $x_0 = \cos\theta_0$. When $\theta_0 = \pi$, the motion is unrestricted and one recovers the isotropic rotor relationship, $\tau_e = 1/6D_w$. In the limit of small θ_0, eq 20 reduces to a much simpler form,

$$D_w\tau_e \approx 7\theta_0^2/24 \qquad (21)$$

where θ_0 is in radians. This approximation is good for fairly large cone angles: if $\theta_0 = 30°$, the error is less than 10%. Given the narrow cone angles in our systems, eq 21 gives an adequate estimate of the wobbling diffusion constant. These constants are listed in Table IV. In general, the wobbling rate is slightly faster for MC540 than for ODRB. This is in striking contrast to the reorientation of these dyes in alcohol solvents, where the rate of rotational diffusion is slower for MC540 than for ODRB. The rate of wobbling is 4 times slower for MC540 in Triton X-100 micelles than in SDS or DTAB micelles. Similarly, the rate of wobbling is about 3 time slower for ODRB in Triton X-100 micelles than in the ionic surfactant micelles. Consequently, these comparisons reveal that the probes are motionally less restricted in the ionic surfactant micelles than in Triton X-100 micelles. This difference can be partially rationalized in terms of the relative sizes of the micelles. Triton X-100 micelles, being larger than SDS or DTAB micelles, will be more tightly packed than the other two types of micelles.

5. Concluding Remarks

These studies have shown that a detailed picture of the structure and dynamics at the micelle–water interface can be gleaned from the time-resolved FDP of lipophilic ionic probes, when the two-step model, in conjunction with the wobbling-in-cone model, is used to analyze the biexponential anisotropy decays. The fact that these models give structural and dynamical parameters that are physically reasonable and that compare well with those obtained in NMR spin relaxation measurements lends credence to this picture. In particular, the fast correlation time associated with the internal motions and the high values of the order parameter are consistent with the probes being located at the surfaces of the micelles. It is also significant that lateral diffusion constants D_L for these probes can be calculated from the parameters of the biexponential fits. The agreement of the values of the lateral diffusion constants obtained from the FDP and NMR measurements provides independent confirmation of the two-step model for describing dynamics in micelles. Finally, lateral diffusion provides another means of understanding probe–micelle interactions. It could also play an important role in electron-transfer and excitation energy transport processes in micelles. These latter two issues will be further explored in our laboratories.

Acknowledgment. E.L.Q. thanks the National Institutes of Health (R15-GM42192-01) and the Robert A. Welch Foundation (D-1019) for supporting this research. A.H.M. and M.D.F. thank the Department of Energy, Office of Basic Energy Sciences (DE-FG03-84ER13251) for supporting this research. We all thank the Stanford Center for Materials Research Polymer Thrust Program for support of the picosecond fluorescence apparatus.

References and Notes

(1) Fendler, J. H. *Membrane Mimetic Chemistry*; Wiley-Interscience: New York, 1982.
(2) *Solution Chemistry of Surfactants*; Mittal, K. L., Ed.; Plenum Press: New York, 1979; Vols. 1 and 2.
(3) Armstrong, D. W. *Sep. Purif. Methods* **1985**, *14*, 213.
(4) Grieser, F.; Drummond, C. J. *J. Phys. Chem.* **1988**, *92*, 5580.
(5) Berne, B. J.; Pecora, R. *Dynamic Light Scattering*; Wiley: New York, 1976.
(6) Shinitzky, M.; Dianoux, A.-C.; Gitler, C.; Weber, G. *Biochemistry* **1971**, *10*, 2106.
(7) Dorrance, R. C.; Hunter, T. F. *J. Chem. Soc., Faraday Trans. 1* **1972**, *68*, 1312.
(8) Grätzel, M.; Thomas, J. K. *J. Am. Chem. Soc.* **1973**, *95*, 6885.
(9) Chen, M.; Grätzel, M.; Thomas, J. K. *J. Am. Chem. Soc.* **1975**, *97*, 2052.
(10) Klein, U. K. A.; Haar, H.-P. *Chem. Phys. Lett.* **1978**, *58*, 531.
(11) Lessing, H. E.; Von Jena, A. *Chem. Phys.* **1979**, *41*, 395.
(12) Rice, S. A.; Kenney-Wallace, G. A. *Chem. Phys.* **1980**, *47*, 161.
(13) Reed, W.; Politi, M. J.; Fendler, J. H. *J. Am. Chem. Soc.* **1981**, *103*, 4591.
(14) (a) Blatt, E.; Ghiggino, K. P.; Sawyer, W. H. *J. Phys. Chem.* **1982**, *86*, 4461. (b) Blatt, E.; Ghiggino, K. P.; Sawyer, W. H. *Chem. Phys. Lett.* **1985**, *114*, 47.
(15) Visser, A. J. W. G.; Vos, K.; van Hoek, A.; Santema, J. S. *J. Phys. Chem.* **1988**, *92*, 759.
(16) (a) Chou, S.-H.; Wirth, M. J. *J. Phys. Chem.* **1989**, *93*, 7694. (b) Wirth, M. J.; Chou, S.-H.; Piasecki, D. A. *Anal. Chem.* **1991**, *63*, 146.
(17) (a) Easton, T. G.; Valinsky, J. E.; Reich, E. *Cell* **1978**, *13*, 476. (b) Valinsky, J. E.; Easton, T. G.; Reich, E. *Cell* **1978**, *13*, 487.
(18) Lelkes, P. I.; Miller, I. R. *J. Membr. Biol.* **1980**, *52*, 1.
(19) (a) Williamson, P.; Massey, W. A.; Phelps, B. M.; Schlegel, R. A. *Mol. Cell. Biol.* **1981**, *1*, 128. (b) Williamson, P.; Mattocks, K.; Schlegel, R. A. *Biochim. Biophys. Acta* **1983**, *732*, 387.
(20) (a) Verkman, A. S.; Frosch, M. P. *Biochemistry* **1985**, *24*, 7117. (b) Verkman, A. S. *Biochemistry* **1987**, *26*, 4050.
(21) Guarcello, V.; Stern, A.; Rizza, V. *Biochim. Biophys. Acta* **1987**, *917*, 318.
(22) (a) Dodin, G.; Aubard, J.; Falque, D. *J. Phys. Chem.* **1987**, *91*, 1166. (b) Dodin, G.; Dupont, J. *J. Phys. Chem.* **1987**, *91*, 6322.
(23) (a) Waggoner, A. *J. Membr. Biol.* **1976**, *27*, 317. (b) Waggoner, A. *Annu. Rev. Biophys. Bioeng.* **1979**, *8*, 47. (c) Waggoner, A. S.; Grinvald, A. *Ann. N.Y. Acad. Sci.* **1977**, *303*, 217. (d) Waggoner, A. S. *Methods Enzymol.* **1979**, *55*, 689.
(24) Salama, G.; Morad, M. *Science* **1976**, *191*, 485.
(25) Tasaki, I.; Warashina, A. *Photochem. Photobiol.* **1976**, *24*, 191.
(26) Dragsten, P. R.; Webb, W. W. *Biochemistry* **1978**, *17*, 5228.
(27) Sieber, F.; Spivak, J. L.; Sutcliffe, A. M. *Proc. Natl. Acad. Sci. U.S.A.* **1987**, *84*, 2999.
(28) (a) Kalyanaraman, B.; Feix, J. B.; Sieber, F.; Thomas, J. P.; Girotti, A. W. *Proc. Natl. Acad. Sci. U.S.A.* **1987**, *84*, 2999. (b) Feix, J. B.; Kalyanaraman, B. *Photochem. Photobiol.* **1991**, *53*, 39. (c) Feix, J. B.; Kalyanaraman, B. *Arch. Biochem. Biophys.* **1991**, *1*, 43.
(29) Gaffney, D. K.; O'Brien, J.; Sieber, F. *Photochem. Photobiol.* **1991**, *53*, 85.
(30) (a) Davila, J.; Gulliya, K. S.; Harriman, A. *J. Chem. Soc., Chem. Commun.* **1989**, 1215. (b) Davilia, J.; Harriman, A.; Gulliya, K. S. *Photochem. Photobiol.* **1991**, *53*, 1.
(31) (a) Ediger, M. D.; Domingue, R. P.; Fayer, M. D. *J. Chem. Phys.* **1984**, *80*, 1246. (b) Marcus, A. H.; Diachun, N. A.; Fayer, M. D. *J. Phys. Chem.* **1992**, *96*, 8930.
(32) Johansson, L. B.-A.; Niemi, A. *J. Phys. Chem.* **1987**, *91*, 3020.
(33) Holowka, D.; Baird, B. *Biochemistry* **1983**, *22*, 3475.
(34) Hoekstra, D.; de Boer, T.; Klappe, K.; Wilschut, J. *Biochemistry* **1984**, *23*, 5675.
(35) (a) Robson, R. J.; Dennis, E. A. *J. Phys. Chem.* **1977**, *81*, 1075. (b) Corti, M.; Degiorgio, V. *J. Phys. Chem.* **1981**, *85*, 1142.
(36) Fendler, J. H. *Acc. Chem. Res.* **1976**, *9*, 153.
(37) Briggs, J.; Nicoli, D. F.; Ciccolello, R. *Chem. Phys. Lett.* **1980**, *73*, 149.
(38) Tanford, C. *J. Phys. Chem.* **1972**, *21*, 3020.
(39) Lianos, P.; Zana, R. *J. Colloid Interface Sci.* (a) **1981**, *84*, *100*; (b) **1982**, *88*, 594.
(40) Stein, A. D.; Peterson, K. A.; Fayer, M. D. *J. Chem. Phys.* **1990**, *92*, 5622.
(41) O'Conner, D. V.; Phillips, D. *Time-Correlated Single Photon Counting*; Academic Press: London, 1984.
(42) Flom, S. R.; Fendler, J. H. *J. Phys. Chem.* **1988**, *92*, 5908.
(43) Tao, T. *Biopolymers* **1969**, *8*, 609.
(44) Chuang, T. J.; Eisenthal, K. B. *J. Chem. Phys.* **1972**, *57*, 5094.
(45) Quitevis, E. L.; Horng, M.-L. *J. Phys. Chem.* **1990**, *94*, 5684.
(46) Debye, P. *Polar Molecules*; Dover: New York, 1929; pp 77–85.
(47) Nee, T.-W.; Zwanzig, R. *J. Chem. Phys.* **1970**, *52*, 6353.
(48) Hubbard, J. B.; Wolynes, P. G. *J. Chem. Phys.* **1978**, *69*, 998.
(49) Madden, P.; Kivelson, D. *J. Chem. Phys.* **1982**, *86*, 4244.
(50) Dote, J. L.; Kivelson, D.; Schwartz, R. N. *J. Phys. Chem.* **1981**, *85*, 2169.
(51) Mukerjee, P.; Cardinal, J. R. *J. Phys. Chem.* **1978**, *82*, 1620.
(52) McIntire, G.; Chiappardi, D. M.; Casselberry, R. L.; Blount, H. N. *J. Phys. Chem.* **1982**, *86*, 2632.
(53) Christensen, R. L.; Drake, R. C.; Phillips, D. *J. Phys. Chem.* **1986**, *90*, 5960.
(54) Kinoshita, J.; Kawato, S.; Ikegami, A. *Biophys. J.* **1977**, *20*, 289.
(55) (a) Lipari, G.; Szabo, A. *Biophys. J.* **1980**, *30*, 489. (b) Lipari, G.; Szabo, A. *J. Chem. Phys.* **1981**, *75*, 2971. (c) Lipari, G.; Szabo, A. *J. Am. Chem. Soc.* **1982**, *104*, 4546. (d) Szabo, A. *J. Chem. Phys.* **1984**, *81*, 1984.
(56) Wang, C. C.; Pecora, R. *J. Chem. Phys.* **1980**, *72*, 5333.
(57) Fujiwara, T.; Nagayama, K. *J. Chem. Phys.* **1985**, *83*, 3110.
(58) Martinez, M. C. L.; de la Torre, J. G. *Biophys. J.* **1987**, *52*, 303.
(59) Wennerström, H.; Lindman, B.; Söderman, Drakenberg, T.; Rosenholm, J. B. *J. Am. Chem. Soc.* **1979**, *101*, 6860.
(60) (a) Ahläs, T.; Söderman, O.; Hjelm, C.; Lindman, B. *J. Phys. Chem.* **1983**, *87*, 822. (b) Walderhaug, H.; Söderman, O.; Stilbs, P. *J. Phys. Chem.* **1984**, *88*, 1655. (c) Néry, H.; Söderman, O.; Canet, D.; Walderhaug, H.; Lindman, B. *J. Phys. Chem.* **1986**, *90*, 5802.
(61) For recent reviews see: (a) Nakagawa, T.; Tokiwa, F. *Surf. Colloid Sci.* **1976**, *6*, 69. (b) Wennerström, H.; Lindman, B. *Phys. Rep.* **1979**, *52*, 1.
(62) Doi, M.; Edwards, S. F. *Theory of Polymer Dynamics*; Clarendon Press: New York, 1986; pp 290–291.
(63) Houslay, M. D.; Stanley, K. K. *Dynamics of Biological Membranes*; Wiley: New York, 1982; pp 39–91.
(64) Silver, B. L. *The Physical Chemistry of Membranes*; Solomon Press: New York, 1985; pp 75–109, 231–247.
(65) Hartley, G. S. *J. Chem. Soc.* **1938**, 1968.
(66) Benjamin, L. *J. Phys. Chem.* **1966**, *70*, 3790.
(67) Waggoner, A. S.; Griffith, O. H.; Christensen, C. P. *Proc. Natl. Acad. Sci. U.S.A.* **1967**, *57*, 1198.
(68) Rosenholm, J. B.; Drakenberg, T.; Lindman, B. *J. Colloid Interface Sci.* **1978**, *63*, 538.